



Microwave properties of $\text{Ba}(\text{Zn}_{1/3}\text{Ta}_{2/3})\text{O}_3$ dielectric resonators

L. Nedelcu*, M.I. Toacsan, M.G. Banciu, A. Ioachim

National Institute of Materials Physics, 077125 Bucharest-Magurele, Romania

ARTICLE INFO

Article history:

Received 21 July 2010

Received in revised form 7 September 2010

Accepted 8 September 2010

Available online 22 September 2010

Keywords:

Barium zinc tantalate

Solid-state reaction

Dielectric resonators

Microwaves

ABSTRACT

$\text{Ba}(\text{Zn}_{1/3}\text{Ta}_{2/3})\text{O}_3$ (BZT) dielectric resonators were prepared by solid-state reaction. The starting materials were BaCO_3 , ZnO , and Ta_2O_5 powders with high purity. The double calcined BZT pellets were sintered in air at temperatures of 1575, 1600, 1625, and 1650 °C for 4 h. The X-ray diffraction data allowed the study of the unit cell distortion degree and the presence of the secondary phases. A long-range order with a 2:1 ratio of Ta and Zn cations on the octahedral positions of the perovskite structure was observed with the increase of the sintering temperature. The dielectric constant of BZT resonators measured around 6 GHz was between 26 and 28. High values of $Q \times f$ product (120 THz) were obtained for BZT resonators sintered at 1650 °C/4 h. The temperature coefficient of the resonance frequency exhibits positive values less than 6 ppm/°C. The achieved dielectric parameters recommend BZT dielectric resonators for microwave and millimeter wave applications.

© 2010 Elsevier B.V. All rights reserved.

1. Introduction

Dielectric materials continue to have a decisive influence on the evolution of the electrical and electronic engineering, communications and information technology. These materials, which exhibit high dielectric constant, low dielectric losses, and good temperature stability are required to reduce the size and weight of equipment, enhance its reliability, and lower the manufacturing and operational costs [1–9]. Ceramics are from far the most utilized as they offer cost-effective solutions for applications.

The $\text{Ba}(\text{Zn}_{1/3}\text{Ta}_{2/3})\text{O}_3$ (BZT) dielectric resonators are known to exhibit a high dielectric constant (ϵ_r), a small temperature coefficient of resonance frequency (τ_f) and a high quality factor (Q). All of these properties are important for the applications of BZT ceramics to microwave devices, in satellite broadcasting and as a high Q dielectric resonator, in mobile phone base stations or combiner filter for Personal Communication System applications [2,10,11].

The factors influencing Q values of BZT have been considered to be long-range ordering (LRO) of cations, zinc oxide evaporation, point defects and stabilization of microdomain boundaries [12,13]. This explained the high Q values from the point of view of its hexagonal superstructure. Sagala and Nambu [14] calculated the dielectric loss tangent at microwave frequencies from the equation of ion motions, which was a function of B-site ordering. Gallasso and Pyle [15] concluded that the B-site ordering increased as the difference in charge and size between B' and B'' atoms increased. Reaney

et al. [16,17] studied the order–disorder transition in BZT using XRD and TEM. They found that the reversible order–disorder phase transition in BZT occurs between 1600 and 1625 °C. The cation ordering in $\text{Ba}(\text{Zn}_{1/3}\text{Ta}_{2/3})\text{O}_3$ complex perovskite is important because the 1:2 ordering along (1 1 1) direction is closely related to the high- Q property of BZT. There is a strong correlation between LRO, domain growth, zinc loss and microwave dielectric parameters.

As a result of our previous investigations, high- Q BZT dielectric resonators ($Q \sim 17,000$ at 5.6 GHz) were achieved by solid-state reaction [18,19]. The aim of this work is a further increase of the quality factor. Four sintering temperatures (1575, 1600, 1625, 1650 °C) were used in order to determine the structural and morphological changes that occur in BZT resonators as a function of sintering temperature, and to use the data obtained to explain the changes in the microwave dielectric properties.

2. Experimental

$\text{Ba}(\text{Zn}_{1/3}\text{Ta}_{2/3})\text{O}_3$ samples were prepared by solid-state reaction. The starting materials were high purity BaCO_3 , ZnO and Ta_2O_5 powders. Stoichiometric quantities were weighted, ground, homogenized and milled in an agate mill in water for 5 h. The powders were calcined at $T = 1200$ °C for 2 h. Then the powders were milled for 3 h and calcined at 1250 °C/2 h. The double calcined powders were mixed with 12% polyvinyl alcohol (PVA) and dried at 80 °C, then were pressed into cylindrical samples of 12 mm diameter and 10 mm height. The pellets were slowly dried at 180 °C in order to eliminate the PVA. The density of green ceramics was $\rho = 4.3$ g/cm³. The sintering treatment for the BZT dielectric resonators was performed in air for 4 h at temperatures of 1575 °C, 1600 °C, 1625 °C and 1650 °C. The samples were polished in order to remove the superficial zone with low Zn content and to obtain correct values of the microwave dielectric parameters.

The bulk densities of the sintered pellets were measured by using a water immersion technique. The structure of BZT samples was investigated by X-ray diffraction (XRD) using a Bruker-D8 ADVANCE type X-ray diffractometer, in focusing geometry, equipped with copper target X-ray tube and LynxEye one-dimensional

* Corresponding author at: National Institute of Materials Physics, P.O. Box MG-7, 077125 Bucharest-Magurele, Romania. Tel.: +40 213690170; fax: +40 213690177.
E-mail address: nedelcu@infim.ro (L. Nedelcu).

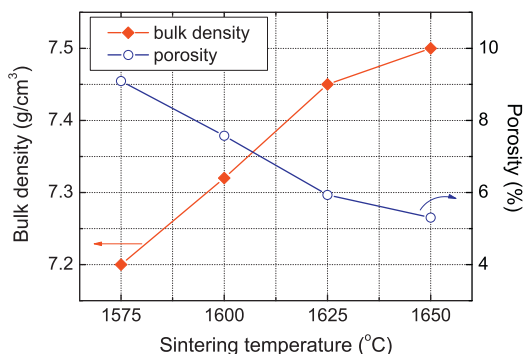


Fig. 1. Bulk density and porosity of BZT samples versus sintering temperature.

detector. The XRD calculations were performed using a Bruker Difractplus Basic Evaluation Package v.12. A corundum plate NIST reference material (NIST SRM 1976) was used for checking the 2θ calibration of the instrument in order to make correct unit-cell parameter calculation and to subtract the effect of the instrumental line width from the line broadening, when calculate the crystallite size. The patterns were recorded at room temperature. The grain morphology and porous structure were analyzed by using a HITACHI S2600N Electronic Microscope.

The low frequency measurements were carried out using a broadband Alpha Analyzer from Novocontrol. The sample was placed in a parallel plate capacitor and the temperature was controlled using a Quatro Cryosystem. In order to diminish the error in relative dielectric constant value measurements, a gold metal film was evaporated on both sides of the sample surface. Capacitance was recorded at 1 MHz in a temperature range between -20 and $+80$ °C. The data were acquired under nearly isothermal conditions ($\Delta T_{\max} = 0.1$ °C) and through a series of ascending temperatures (5 °C steps).

In microwaves, the BZT cylindrical samples exhibit very low dielectric loss, high relative dielectric constant, and a very good stability with temperature. Therefore, the dielectric parameters of BZT samples were investigated by using the Hakki–Coleman method [20]. A computer-aided measurement system, which combines an HP 8757C network analyzer and an HP 8350B sweep oscillator, was employed for the microwave measurements. The temperature coefficient of the resonant frequency τ_f in the microwave range was measured by heating the samples from $+20$ °C to $+80$ °C.

3. Results and discussion

The bulk densities of the fired BZT ceramics were measured after grinding and polishing. The temperature dependence of the densification after sintering treatment in air for 4 h is shown in Fig. 1. The X-ray density of BZT compound with stoichiometric composition was considered as $\rho = 7.94 \text{ g/cm}^3$ [4]. The BZT samples sintered between 1575 and 1650 °C exhibit bulk density greater than 90% of theoretical density. The bulk density slightly increases with the increase of sintering temperature T_s . The best densified ceramics ($T_s = 1650$ °C) exhibit a porosity value of about 5.2%.

Crystallinity and cation ordering of BZT samples were investigated by using powder X-ray diffraction. The diffraction diagrams were recorded in Bragg–Brentano geometry from 15 to $80^\circ 2\theta$ with 0.01° steps and 7 s counting time. The mean crystallite size, D was estimated with the Scherrer equation:

$$D(\text{nm}) = \frac{0.9\lambda(\text{nm})}{\beta \cos \theta} \quad (1)$$

where β is the full width at half maximum and θ is the Bragg angle. The entire peak broadening was attributed only to the crystallite size effect. The line width was corrected for the instrumental broadening using the above mentioned reference sample. The crystallite size was determined after the subtraction of $K_{\alpha 2}$ line from the $K_{\alpha 1} - K_{\alpha 2}$ doublet.

The X-ray diffraction patterns for BZT samples, sintered at 4 temperatures values are given in Fig. 2. The XRD patterns confirm the formation of the BZT hexagonal structure (space group $P\bar{3}m1$). The $\text{Ba}(\text{Zn}_{1/3}\text{Ta}_{2/3})\text{O}_3$ is the major phase, but there is a small amount

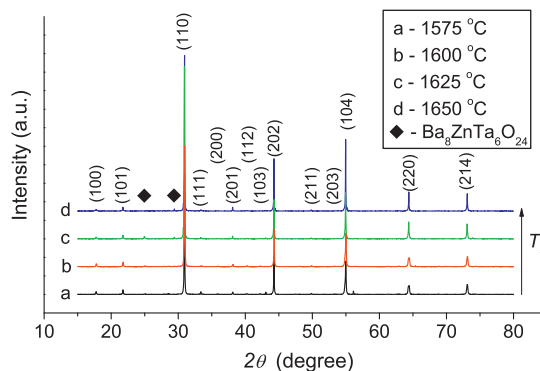


Fig. 2. XRD patterns of BZT samples versus sintering temperature.

of $\text{Ba}_8\text{ZnTa}_6\text{O}_{24}$ formed due to ZnO volatilization during sintering process [21,22].

The structure order was evidenced from the XRD patterns by observing the reflections due to Zn and Ta order (superstructure reflection). The superstructure reflections are related to the amount of Zn and Ta ordering. Therefore, a change in integrated intensity of the superstructure peak corresponds to the amount of Zn and Ta order. The (100) peak has the strongest intensity among the superstructures lines. The XRD computed data reveals the increase in integrated intensity of the (100) diffraction line versus sintering temperature.

Lattice distortion caused by Zn and Ta ordering can be evaluated by the split of the (422) and (226) diffraction peaks. If no distortion occurs, then the (422) and the (226) peaks are not separated. Fig. 3 shows the profile change of (422) and (226) peaks versus sintering temperature. Diffraction patterns show that the ceramics fired up to $T_s = 1625$ °C consist of half distorted and half non-distorted structure. In ceramics fired at 1625 °C, a split of (422) and (226) diffraction peaks can be observed.

The perfectly ordered structure is produced by the following process:

1. A perovskite-type structure is formed, but Zn and Ta are in disorder.
2. Zn and Ta are partially in order.
3. Zn and Ta are completely in order and the lattice is distorted.

At high sintering temperatures, ZnO evaporates and a supplementary distortion can be produced by the ZnO loss [12]. The Zn^{2+} ions on B'-site can be partially replaced by Ba^{2+} . Even though Ba^{2+} have a much larger ionic radius of 1.61 \AA comparatively to 0.74 \AA for Zn^{2+} , the transfer of Ba^{2+} cations for A site to B' site is a possible process [12]. This substitution occurs very slowly and creates

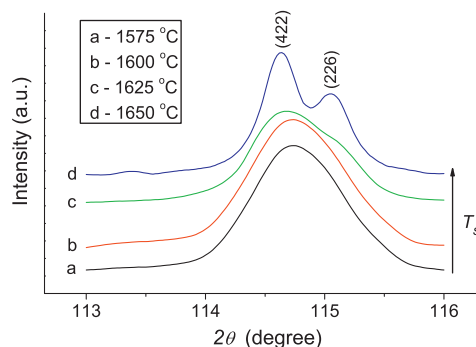


Fig. 3. XRD patterns of BZT samples (detail)—the unit cell distortion as function of T_s .

Table 1
Unit cell parameters and mean crystallite size of BZT samples versus T_s .

Sample	Sintering temperature T_s (°C)	Unit cell parameters			Unit cell volume V_o (Å ³)	Mean crystallite size (nm)
		a_o (Å)	c_o (Å)	c_o/a_o		
BZT 1	1575	5.779	7.086	1.2261	204.94	150
BZT 2	1600	5.777	7.080	1.2255	204.63	155
BZT 3	1625	5.784	7.077	1.2235	205.04	750
BZT 4	1650	5.784	7.074	1.2230	204.95	1300

a supplementary unit cell distortion, even when the LRO is saturated and leads to an increase of Q . The ZnO loss is evidenced in Fig. 2, where the X-ray diffraction patterns indicate the appearance of $Ba_8ZnTa_6O_{24}$ secondary phase, especially at BZT sample surface. Inside the ceramic, the amount of $Ba_8ZnTa_6O_{24}$ secondary phase is very small and does not affect the stoichiometry and dielectric properties of the BZT resonator.

A continuously decrease of the c_o/a_o rapport and the decrease of c_o with the increase of the sintering temperature is shown in Table 1. Moreover, high values of a_o for temperatures higher then 1625 °C can be observed. These data indicate the increase of the unit cell distortion with the increase in T_s . In the same time, a spectacular increase from 150 nm to 1300 nm of mean crystallite size with the increase in sintering temperature can be observed from Table 1.

The microstructure of BZT ceramics sintered in air at 1575–1650 °C/4 h was investigated by using scanning electron microscopy (SEM). The SEM images are presented in Figs. 4a–d. The micrograph of BZT sample sintered at 1575 °C (Fig. 4a) presents a sharp distribution of the grain size. The grains with size in the range 0.5–2 µm are spherical and not well faceted. The porous structure is represented by intergranular pores with size up to 5 µm. At $T_s = 1600$ °C, a growth of spherical grains up to 4 µm occurs, as shown in Fig. 4b. The porosity is reduced and the pores exhibit dimensions between 1 µm and 3 µm. The general morphologic

aspect of BZT samples sintered at 1625 °C changes. Fig. 4c indicates a bimodal grain size distribution, with small grains near 2 µm and bigger ones near 6–7 µm. The intergrain porosity is small, only pores with size in the interval 0.5–2 µm are present. Well faceted, polyhedral grains with smooth surfaces and edges showing dimensions in the range (5–20) µm are observed for BZT sample sintered at 1650 °C (Fig. 4d). The porous structure is represented by sub-micron intergranular pores. The difference between the 1575 °C and 1650 °C sintering temperatures has as effect a strong granular growth, as can be noticed in Figs. 4a–d. This result is in good agreement with the X-ray calculated data for mean crystallite size.

Complex perovskite ceramics with high permittivity and low dielectric loss are used as dielectric resonators at microwave frequencies. The resonance frequency f_o is related to the relative dielectric constant ϵ by the following equation:

$$f_o \approx \frac{c}{\lambda_d \epsilon^{1/2}} \approx \frac{c}{D \epsilon^{1/2}} \quad (2)$$

where c is the speed of light in a vacuum and λ_d is the wavelength of the standing wave along the diameter D of the resonator. One of the most important characteristics for this type of dielectric material is the temperature coefficient of the resonance frequency f_o of a

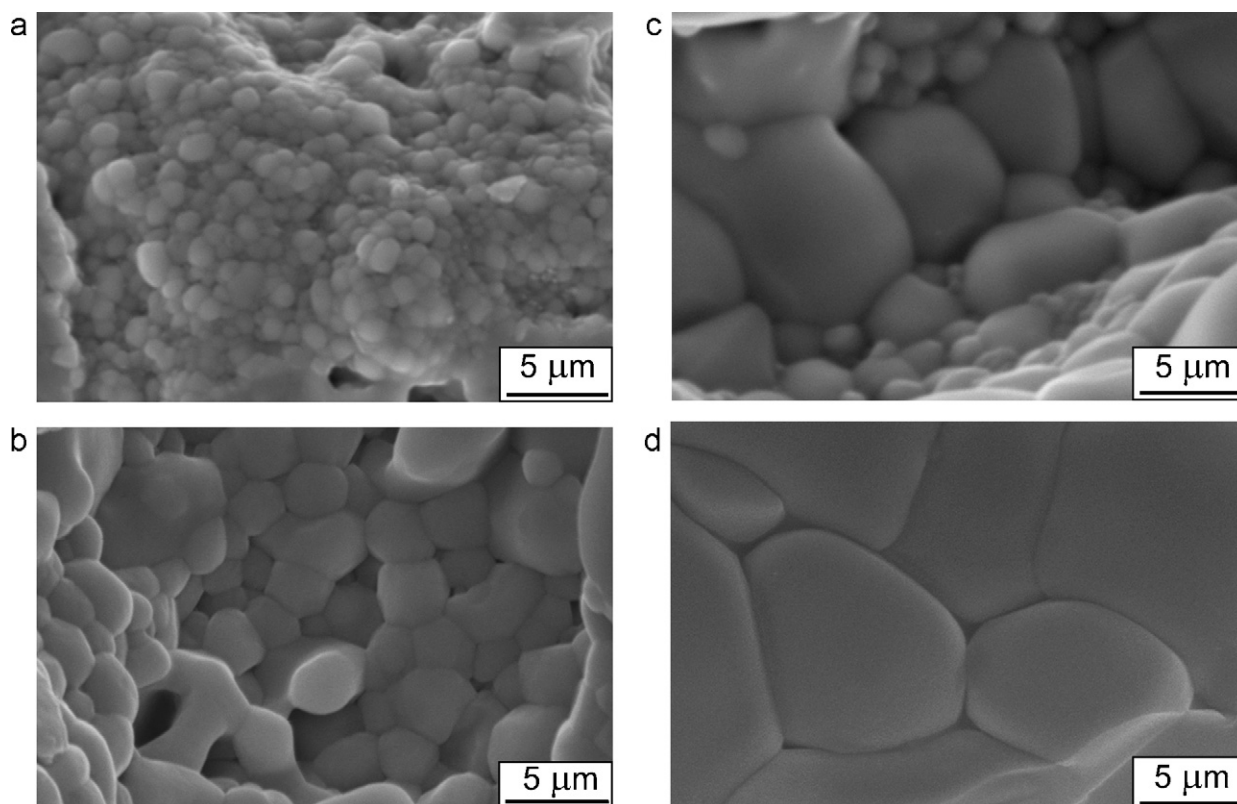


Fig. 4. SEM micrographs of BST ceramics (fracture) for different sintering temperatures: (a) 1575 °C; (b) 1600 °C; (c) 16250 °C; (d) 1650 °C.

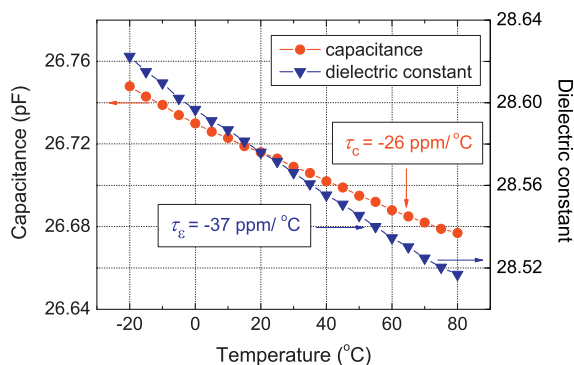


Fig. 5. Capacitance and calculated dielectric constant ε versus temperature for BZT sample sintered at 1650 °C/4 h.

dielectric resonator, which is defined by

$$\tau_f = \frac{1}{f_0} \frac{\partial f_0}{\partial T} \quad (3)$$

Courtney [23] observed a small linear change of the ε in a range of temperatures 10–100 °C for many dielectric materials, in which case, from the above equations, the temperature coefficient τ_f can be approximated by:

$$\tau_f = \frac{1}{f_0^{RT}} \frac{\Delta f_0}{\Delta T} \quad (4)$$

where Δf_0 is the variation in the resonance frequency for a temperature variation ΔT and f_0^{RT} is the value of f_0 at room temperature. In fact, the usual method to determine τ_f is to measure shift of f_0 for the resonator placed in a thermostatic chamber.

In most civil applications, a minimum variation of the material characteristics with the temperature in a range of 40–50 °C around room temperature is required. In order to determine the temperature behaviour of the relative dielectric constant for BZT ceramics, the well-densified samples sintered at 1650 °C were chosen for measurements. The BZT disks were polished and gold electrodes were deposited on the plane-parallel surfaces. The temperature dependence of the capacitance for a BZT capacitor recorded at 1 MHz is presented in Fig. 5. The capacitance shows only a small variation in the –20 to +80 °C temperature interval. For this small variation in capacitance, the dependence of the relative dielectric permittivity on the temperature was calculated from the model of planar capacitor by taking into account the temperature expansion of the sample, $\alpha = 10 \text{ ppm/}^\circ\text{C}$ [4]; the ε values versus the temperature are also presented in Fig. 5. Moreover, the temperature coefficient of the capacitance τ_c and temperature coefficient of the relative dielectric permittivity τ_ε determined by linear fitting on the data are inserted in Fig. 5.

Microwave measurements on dielectric constant and quality factor Q were carried out on the BZT dielectric resonators. For polar dielectric resonators, in the microwave domain, the product between the resonance frequency f and quality factor Q is constant [10]. Due to this fact, the $Q \times f$ product is more used as resonator parameter rather than quality factor. The increase of the dielectric constant and $Q \times f$ product with the increase of the sintering temperature can be observed in Fig. 6. The increase of the dielectric constant can be considered as an effect of the reduced porosity resulting in a better densification of BZT samples at high sintering temperatures. On the other hand, it can be supposed that the dielectric loss due to the pores does not vary too much for these small variation of the porosity (Fig. 1). Therefore, the $Q \times f$ strongly depends on the BZT crystalline structure, that is, on the unit cell distortion and LRO. Highest $Q \times f$ product is obtained for a BZT ceramic with Zn and Ta completely ordered and with a strongly

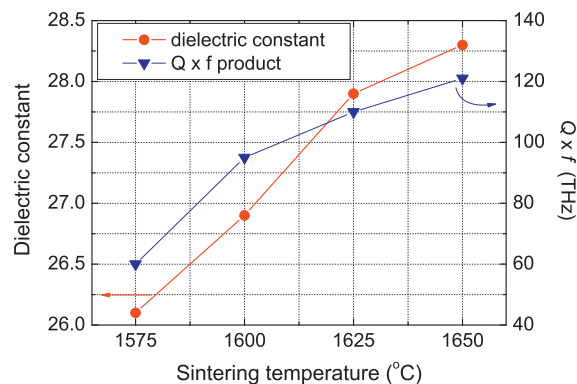


Fig. 6. Dielectric constant and $Q \times f$ product versus T_s for BZT resonators.

distorted unit cell [13,14,24,25]. The best $Q \times f$ value (120 THz) was achieved for BZT resonators sintered at 1650 °C/4 h. These results are in agreement with X-ray diffraction and SEM data. As can be seen in Fig. 3 and Table 1, BZT samples sintered at 1650 °C exhibit the highest unit cell distortion. Moreover, these samples exhibit the largest grain size (Fig. 4d).

An increase in $Q \times f$ values from 75 THz [19] to 100 THz [18] was previously observed due to a increase in the Ta_2O_5 raw material purity from 99.8% to 99.95%. The very high $Q \times f$ values up to 120 THz were achieved in this paper for a 99.95% purity Ta_2O_5 raw material and for a sintering time increased from 2 h [18,19] to 4 h. The 120 THz achieved in this work for $Q \times f$ is in the same range of previously reported values, which were obtained at longer sintering times and with supplementary annealing treatments [4].

Based on the linear dependence of the dielectric permittivity on the temperature, which was observed at low frequency measurements (Fig. 5), the temperature coefficient of the resonant frequency τ_f in microwave range was measured by heating the samples from +20 °C to +80 °C. The BZT dielectric resonators exhibit a positive temperature coefficient of the resonance frequency τ_f in the 3–6 ppm/°C range. The relation between temperature coefficient of the resonance frequency τ_f and temperature coefficient of the capacitance τ_c is [11]:

$$\tau_f + \frac{1}{2} \tau_c + \frac{1}{2} \alpha = 0 \quad (5)$$

where α is the linear thermal-expansion coefficient. Using the above equation for $\alpha = 10 \text{ ppm/}^\circ\text{C}$ [4], the temperature dependence of the capacitance at 1 MHz allowed an estimation of $\tau_f \sim 8 \text{ ppm/}^\circ\text{C}$, which is in a good agreement with microwave measurements.

The high values of $Q \times f$ product obtained for BZT resonators sintered at 1650 °C/4 h recommend this type of materials for applications in microwave communication systems and millimeter wave technology.

4. Conclusions

$\text{Ba}(\text{Zn}_{1/3}\text{Ta}_{2/3})\text{O}_3$ ceramic materials with high dielectric constant and low loss in microwave domain were achieved by solid-state reaction in the temperature range 1575–1650 °C for 4 h.

The XRD patterns confirm the formation of the BZT materials with hexagonal structure. For sintering temperatures higher than 1625 °C, the XRD patterns reveal the formation of a secondary phase with low Zn content.

Low frequency measurements at 1 MHz showed a slow decrease of the dielectric constant with the increase of the temperature. The temperature coefficient τ_ε of the dielectric permittivity was estimated to be –37 ppm/°C.

The dielectric permittivity and the $Q \times f$ product increase with the increasing of the sintering temperature. The temperature coefficient τ_f of the resonance frequency exhibits positive values less than 6 ppm/°C.

Well-sintered BZT resonators exhibit a dielectric constant around 28 and a $Q \times f$ product up to 120,000 GHz. The achieved high values of the quality factor Q recommend the BZT materials for microwave and millimeter wave applications.

Acknowledgments

This work was supported by the Ministry of Education and Research of Romania through the Core Program PN09-45 and the project PNII 12-078/2008. The authors thank to Dr. Sorin Jinga from the University “Politehnica” of Bucharest for SEM investigations. The authors are also grateful to Paul Ganea from the National Institute of Materials Physics for his help in low frequency measurements.

References

- [1] R.J. Cava, J. Mater. Chem. 11 (2001) 54–62.
- [2] S.J. Fiedziuszko, I.C. Hunter, T. Itoh, Y. Kaobayashi, T. Nishikawa, K. Wakino, S.N. Stitzer, IEEE Trans. Microw. Theory Tech. MTT 50 (2002) 706–720.
- [3] A. Ioachim, M.G. Banciu, L. Nedelcu, C.A. Dutu, J. Optoelectron. Adv. Mater. 8 (2006) 941–943.
- [4] M.T. Sebastian, Dielectric Materials for Wireless Communication, Elsevier Ltd., 2008.
- [5] X. Lu, Y. Lee, S. Yang, Y. Hao, R. Ubic, J.R.G. Evans, C.G. Pariniy, J. Am. Ceram. Soc. 92 (2009) 371–378.
- [6] S. Genovesi, F. Costa, B. Cioni, V. Miceli, G. Annino, G. Gallone, G. Levita, A. Lazzeri, A. Monorchio, G. Manara, Microw. Opt. Technol. Lett. 51 (11) (2009) 2753–2758.
- [7] Y.-C. Chen, S.-M. Tsao, C.-S. Lin, S.-C. Wang, Y.-H. Chien, J. Alloys Compd. 471 (2009) 347–351.
- [8] Y.-C. Chen, S.-L. Yao, R.-J. Tsai, K.-C. Chen, J. Alloys Compd. 486 (2009) 410–414.
- [9] H. Zhou, X. Chen, L. Fang, C. Hu, J. Am. Ceram. Soc. 93 (2010) 1537–1539.
- [10] T. Higuchi, H. Tamura, J. Eur. Ceram. Soc. 23 (2003) 2683–2688.
- [11] Y.M. Reaney, D. Iddles, J. Am. Ceram. Soc. 89 (2006) 2063–2072.
- [12] S. Desu, H.M. O' Bryan, J. Am. Ceram. Soc. 68 (1985) 546–551.
- [13] H. Tamura, D.A. Sagala, K. Wakino, Jpn. J. Appl. Phys. 25 (1986) 787–791.
- [14] D.A. Sagala, S. Nambu, J. Am. Ceram. Soc. 75 (1992) 2573–2575.
- [15] F. Gallasso, J. Pyle, Inorg. Chem. 2 (1983) 482–484.
- [16] I.M. Reaney, I. Qazi, W.E. Lee, J. Appl. Phys. 88 (2000) 6708–6714.
- [17] I. Qazi, I.M. Reaney, W.E. Lee, J. Eur. Ceram. Soc. 21 (2001) 2613–2616.
- [18] A. Ioachim, L. Nedelcu, E. Andronescu, S. Jinga, M.I. Toacsan, M.G. Banciu, A. Lörinczi, M. Popescu, J. Optoelectron. Adv. Mater. 10 (2008) 209–212.
- [19] H.V. Alexandru, A. Ioachim, M.I. Toacsan, L. Nedelcu, M.G. Banciu, C. Berbecaru, G. Voicu, S. Jinga, E. Andronescu, Ann. N. Y. Acad. Sci. 1161 (2009) 549–553.
- [20] B.W. Hakki, P.D. Coleman, IRE Trans. MTT 8 (1962) 402–410.
- [21] S.M. Moussa, J.B. Claridge, M.J. Rosseinsky, S. Clarke, R.M. Ibberson, T. Price, D.M. Iddles, D.C. Sinclair, Appl. Phys. Lett. 82 (2003) 4537–4539.
- [22] M. Thirumal, P.K. Davies, J. Am. Ceram. Soc. 88 (2005) 2126–2128.
- [23] W.E. Courtney, IEEE Trans. Microw. Theory Tech. MTT 18 (1970) 476–485.
- [24] M. Bieringer, S.M. Moussa, L.D. Noailles, A. Burrows, C.J. Kiely, M.J. Rosseinsky, R.M. Ibberson, Chem. Mater. 15 (2003) 586–597.
- [25] H. Tamura, J. Eur. Ceram. Soc. 26 (2006) 1775–1780.